The International Journal of Advanced Manufacturing Technology (2018) 99:2579–2584
https://doi.org/10.1007/s00170-018-2655-9

ORIGINAL ARTICLE

Influence of aluminum silicate stabilizer on the coating structural composition and characteristics of multifunctional developed composite coating: a buildup for defense application

O. S. I. Fayomi[1,2] · A. A. Ayodeji[3] · E. B Omoniyi[4] · S. T. Okolie[2]

Received: 27 April 2018 / Accepted: 29 August 2018 / Published online: 6 September 2018

Abstract
The trajectory challenge of defense component in service is basically as a result of fallout in both structural, plastic deformation, and corrosion vulnerability. In an attempt to address this catastrophe, Zn-SiO_2 composite films were produced on mild steel substrate by electro-deposition route from zinc-based sulfate solutions in the presence $Al_6O_{13}Si_2$ particle. The thin film coating was investigated using scanning electron microscopy coupled with energy dispersive spectroscopy (SEM/EDS). The anti-corrosion behavior in 3.65% NaCl medium was studied using potentiodynamic polarization technique and characterized by high resolution optical microscope (HR-OPM). The wear and the hardness properties of the composite coatings were measured with high diamond microhardness tester and reciprocating sliding tester respectively. Experimental results show that co-deposited $Al_6O_{13}Si_2$ particle provides new orientation of metal matrix and modified the surface structure which contributed maximally to 80% increase in hardness and 40% increase in wear resistance. More so, increase in anti-corrosion property of all the deposits fabricated is attributed to the formation of new surface evolution. This result attested to the fact that this component is suitable for defense application.

Keywords Zn-SiO_2-$Al_6O_{13}Si_2$ · Composite coatings · Thin films · Tribology · Corrosion

1 Introduction

Recently, threat arising from fracture, fatigue, and wear is considered as one of the fundamental challenge facing defense component in service. Specific weapon entrained debris, groove, and reactive erosion leading to severe failure [1–3]. The role of ceramic composite both from traditional and synthesized form in fabrication of highly sophisticated protective surface coverage becomes imperative [4, 5]. Comparatively, electrodeposition techniques are the preferred methods of metal coating due to their bonding characteristics, good texture, high thickness ratio, and low cost [6–8]. The widespread depositions then have been through single coating system of Zn, Ni, Co, and Si to mention but a few on mild steel substrates [9]. Failure obtained has been a result of non-durability in intense corrosive and wear environments and this has affected its effectiveness negatively [10–12]. To address this drawback, composite depositions have been seen as alternative for enhancing zinc coating properties [13–15]. Composite deposition is a unique trend for depositing particles of metallic and non-metallic alloys/compounds in insoluble form or ceramic and polymer forms into electrolytic bath for specific functions, chemical and mechanical properties [15–22]. Evolution of based materials containing composite and ceramics like ZnO, TiO_2, Al_2O_3, Al_6O_{13}, and $C_{r2}O_3$ SiO_2 has proved to give excellent oxidation stability and tribological resistance [23–25]. Though, report on SiO_2 composite particle has been substantial with focus on its corrosion and

✉ O. S. I. Fayomi
ojosundayfayomi3@gmail.com

1 Department of Chemical, Metallurgical and Materials Engineering, Tshwane University of Technology, P.M.B. X680, Pretoria, South Africa

2 Department of Mechanical Engineering, Covenant University, P.M.B 1023, Ota, Ogun State, Nigeria

3 Department of Chemical Engineering, Covenant University, P.M.B 1023, Ota, Ogun State, Nigeria

4 Department of Mechanical Engineering, Bell University of Technology, Ota, Ogun State, Nigeria

morphological behaviors and not on their mechanical resistance properties [26–28]. It is evident that for a material to be beneficial for industrial applications, not only its corrosion behavior likewise its mechanical properties or more precisely its surface dependent properties should be studied [29–31]. In view of this, Zn-SiO_2-$Al_6O_{13}Si_2$ composite coatings through electrolytic deposition will be considered first, followed by the structure characterization, corrosion properties, and the mechanical (hardness and wear) behavior.

2 Experimental procedure

2.1 Preparation of substrates

Mild steel of (40 mm × 20 mm × 1 mm) commercially sourced flat sheet was used as cathode substrate and 99.5% zinc plate of (30 mm × 20 mm × 1 mm) were prepared as anodes. The surface preparation was performed with different grade of emery paper as described in our previous studies [3, 14]. The sample were properly cleaned with sodium carbonate, pickled and activated with 10% HCl at ambient temperature for 10 s, then followed by instant rinsing in deionized water. Table 1 shows the spectrometer chemical analysis of the mild steel substrate used for this study.

2.2 Material composition and formation

Zn-SiO_2-$Al_6O_{13}Si_2$ composite coating was produced in a single cell containing two zinc anode and single cathode electrodes. The distance between the anode and the cathode is 15 mm. All chemical used are analytical grade and deionized water was used in all solution admixed and preheat at 40 °C. The processed parameters and bath composition admixed used for the coating are shown in Tables 2 and 3. The choice of the deposition parameter is in line with the preliminary study and our previous work [22].

The set electrodes were connected to the direct current via a rectifier at applied potential of 0.5 V for 15 min constant time. The plating was done, rinsed in distilled water, and samples were air-dried thereafter sectioned for characterization.

2.3 Characterization of coating

The composite coating obtained was characterized using VEGA TESCAN Scanning electron microscope equipped with EDS. The phase change was verified with XRD. Microhardness studies were carried out using a diamond pyramid indenter EMCO Test Dura-scan 10 microhardness testers at a load of 10 g for a period of 20 s. The microhardness trends (for both heat-treated and untreated samples) were measured across the plated surface in an interval of 20 μm.

Table 1 Chemical composition of mild steel used (wt%)

Element	C	Mn	Si	P	S	Al	Ni	Fe
Composition	0.15	0.45	0.18	0.01	0.031	0.005	0.008	Balance

Table 2 Processed parameter for Zn-SiO_2-$Al_6O_{13}Si_2$ sulfate bath formulation

Composition	Mass concentration (g/L)
$ZnSO_4$	75
$NaSO_4$	15
Boric acid	5
Glycine	5
Thiourea	5
SiO_2	10
$Al_6O_{13}Si_2$	5–15
pH	4.5–5.0
Voltage	0.5
Time	15 min
Temp	40 °C

2.4 Wear tests

The tribological properties of the deposited alloy were measured using CERT UMT-2 multifunctional tribological tester at ambient temperature of 25 °C with schematic diagram as shown in Fig. 2. The reciprocating sliding tests were carried out with the load of 5 N and 10 N, constant speed of 5 mm/s, displacement amplitude of 2 mm in 20 min. A Si_3N_4 ball (4 mm in diameter, HV 50–1600 g) was chosen as counter body for the evaluation of tribological behavior of the coated sample. The dimension of the wear specimen is 2 cm by 1.5 cm as prescribed by the specimen holder. After the wear test, the structure of the wear scar and film worn tracks is further examined with the help of high optic Nikon Optical microscope (OPM) and scanning electron microscope couple with energy dispersive spectroscopy (VEGAS-TESCAN SEM/EDS).

Table 3 Itinerary parameters of Zn-SiO_2-$Al_6O_{13}Si_2$ alloy co-deposition

Sample numbers	Time (min)	Coating thickness (μm)	Weight gain (g)	Coating per unit area (mg/mm^2)
Zn-10SiO_2	15	212.3		0.0419832
Zn-10SiO_2-5$Al_6O_{13}Si_2$	15	184.7	0.24	0.2560880
Zn-10SiO_2-10$Al_6O_{13}Si_2$	15	134.1	0.28	0.0221816
Zn-10SiO_2-15$Al_6O_{13}Si_2$	15	177.7	0.23	0.0358309

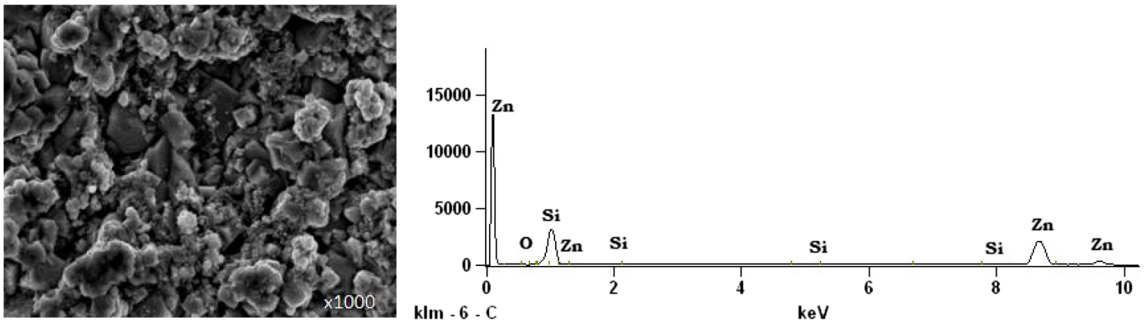

Fig. 1 SEM/EDS of Zn-10SiO_2 coated mild steel showing the surface morphology

2.5 Electrochemical test

Autolab PGSTAT101 Metrohm potentiostat with a three-electrode cell assembly in a 3.65% NaCl static solution at 40 °C was used to examine the anti-corrosion behavior of the composite coatings. The developed composite was the working electrode; platinum electrode was used as counter electrode and Ag/AgCl was used as reference electrode. The anodic and cathodic polarization curves were recorded by a constant scan rate of 0.012 V/s which was rated between − 1.5 and + 1.5 mV.

3 Results and discussion

3.1 SEM/EDS analysis of Zn-SiO_2 deposited mild steel

Figures 1 and 2 show the surface morphology of the Zn-10SiO_2 and Zn-10SiO_2-15$Al_6O_{13}Si_2$ samples. EDS spectra clearly showed the presence of Zn, Si, and O elements (Fig. 1) and Zn, Si, Al, and O elements (Fig. 2) on the mild steel surfaces. From the two figures, it was noticeable that the crystal structure of the deposits in Fig. 2 possesses a stable crystal build up, compared to the distribution observed in Fig. 1. Invariably, the deposited alloys of Zn-10SiO_2-15Al6O_{13}Si2 coating sample were more compact compared to the rest of coating produced with lesser wt% concentration.

No doubt the plated appearance and the coating interface of Zn-10SiO_2-15$Al_6O_{13}Si_2$ were quite good because the nanoceramic particulate strengthens the composite in the zinc metal matrix and swiftly enhances microstructural evolution. The structural behavior was as expected given that the zinc metals are often known as load bearer which invariably supports nucleation propagation. The distribution of the particulate covers the nucleation spot and strengthened the fabricated composite, which is in par with the attested study by [11–13]. More so, from the two figures, it is essential to point out that microstructural change may be due to high particle loading of the $Al_6O_{13}Si_2$ nanoceramic composite resulting in good precipitation and improved orientation. Nevertheless, the potential properties of $Al_6O_{13}Si_2$ with the reactive metal in electrolyte can be term visible since the evidence leading to performance has been justified by the microstructural evolution with percentage inoculation of the particulate in bath.

Optical microscope was used to study the microstructures of the composite samples after heat treatment (Fig. 3). The images were taken at × 100 magnification. It can be seen that, the coating matrix with binary Zn-SiO_2 alloy had little adherence at high temperature as a result of pileup. It was observed that as the concentration of $Al_6O_{13}Si_2$ increases in the formulations, the number of pits begins to disappear and recrystallization occurs. That is, the microstructures were becoming more finely and uniformly, so the addition of more $Al_6O_{13}Si_2$ up to 15 g/L concentration was highly needed. It

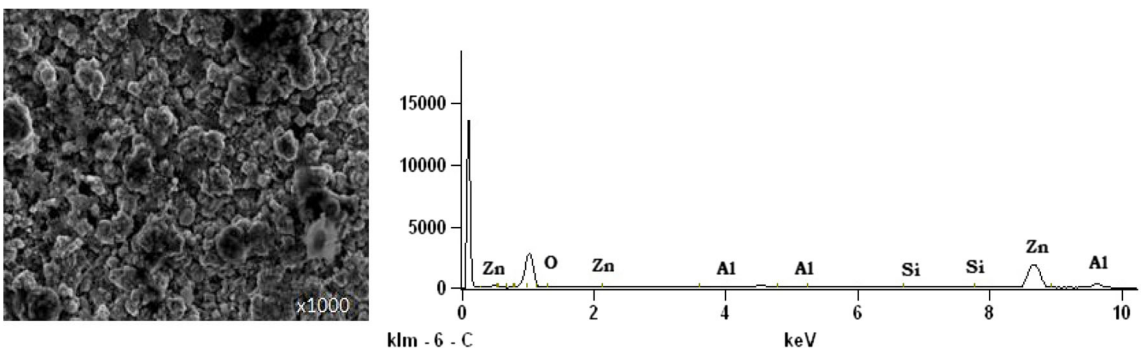

Fig. 2 SEM/EDS of Zn-10SiO_2-15$Al_6O_{13}Si_2$ coated mild steel showing the surface morphology

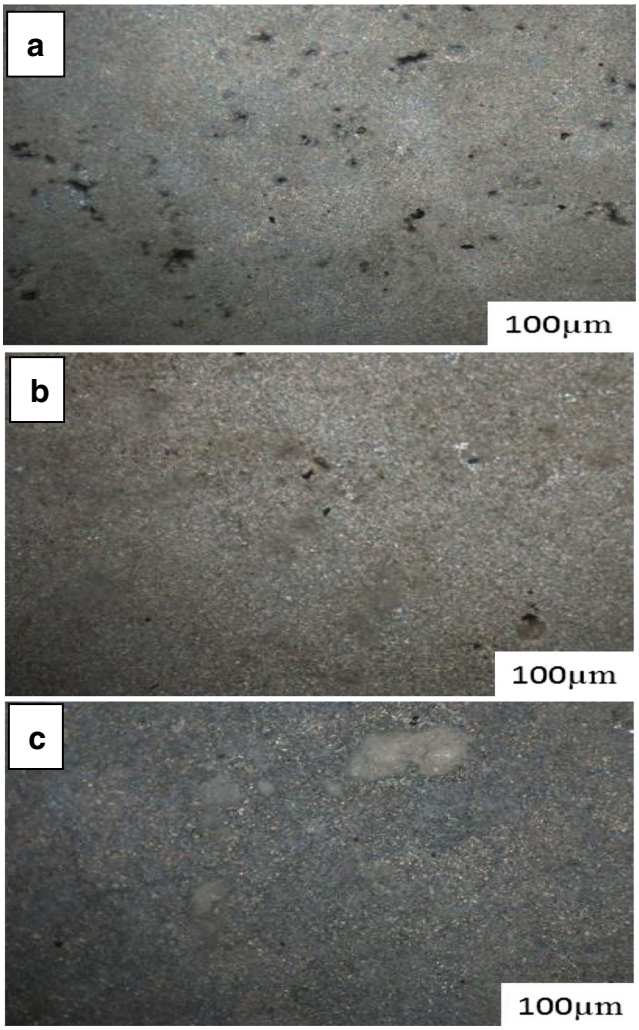

Fig. 3 Optical micrographs of the coated samples after heat treatment. **a** Zn-10SiO_2-5$Al_6O_{13}Si_2$. **b** Zn-10SiO_2-10$l_6O_{13}Si_2$. **c** Zn-10SiO_2-15$Al_6O_{13}Si_2$

can be said that the increase in coating thickness led to less coarse surfaces, as reported by [12]. This observation is in support of the findings obtained from the SEM/EDS analysis.

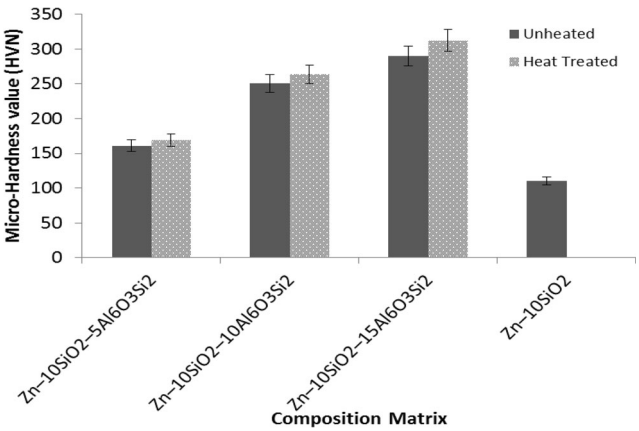

Fig. 4 The microhardness for Zn-SiO_2 samples

3.2 Microhardness analysis of Zn-SiO_2 and Zn-SiO_2-$Al_6O_{13}Si_2$ deposited mild steel

The microhardness results for the Zn-SiO_2 and Zn-SiO_2-$Al_6O_{13}Si_2$ composite coating at various bath composition and parameter are shown in Fig. 4. In all, the deposited composite coatings in all matrixes had good microhardness propagation than Zn-SiO_2 sample. It is identified and noticed that $Al_6O_{13}Si_2$ in the composite coating could act as a strong barrier to disallow deformation of the solid matrix and further enhance the hardness property. Also, increase in the concentration of $Al_6O_{13}Si_2$ composite coating (for both heated and unheated) contributes to the hardness of the coated steel. For instance, increasing the composite concentration (for unheated sample) from 5 to 15 g/L changes the microhardness value from 161 to 290 HVN. As far as hardening behavior of the composites is concerned, particle addition in the matrix alloy increases the strain energy in the periphery of the particles in the matrix [8].

Clearly, it can also be seen that the heat treatment of Zn-SiO_2 and Zn-SiO_2-$Al_6O_{13}Si_2$ composition matrixes impacts on the strengthening tendency and hardness behavior steel substrate. Generally, a report by [16] shows that heat treatment enhances adhesion kinetic of $Al_6O_{13}Si_2$ (a chemically active substance) at the surface of Zn-SiO_2 mild steel. This claim is in line with the descriptive studies made by [8].

3.3 Wear rate evaluation of Zn-SiO_2 and Zn-SiO_2-$Al_6O_{13}Si_2$ deposited mild steel

Figure 5 shows comparative tribological behavior of total wear loss of all matrix composite and Zn-10SiO_2 mild steel substrate. It was observed that the composite coating exhibited significantly higher wear resistance than the Zn-10SiO_2 matrix due to the addition of $Al_6O_{13}Si_2$ which acts as a load-bearing constituent. As the percentage of $Al_6O_{13}Si_2$ increases, the wear rate of the composite coating decreases. Increase in $Al_6O_{13}Si_2$ in Zn-10SiO_2 coating of mild steel restricts the formation of the matrix material with respect to load; hence,

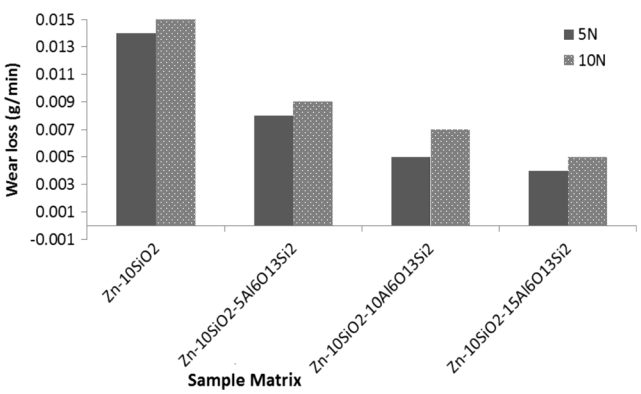

Fig. 5 Variation of the wear rate Zn-SiO_2 deposited mild steel

Table 4 Summary of the potentiodynamic polarization results

Sample	E_{corr} Obs (V)	i_{corr} (A/cm^2)	R_p (Ω)	Corrosion rate (mm/year)
Zn-10SiO_2	− 1.3320	6.04E-03	127.61	0.07000
Zn-10SiO_2-5$Al_6O_{13}Si_2$	− 1.1894	1.48E-04	185.83	0.03108
Zn-10SiO_2-10$Al_6O_{13}Si_2$	− 1.1811	1.31E-04	204.64	0.02196
Zn-10SiO_2-15$Al_6O_{13}Si_2$	− 1.1468	5.10E-05	372.99	0.01123

the wear rate for higher percentage of composite coating is lower. For example, wear rates of 0.014 g/min, 0.008 g/min, and 0.005 g/min were obtained (when a load of 5 N is exerted) for the concentration of 0 g/L, 5 g/L, and 10 g/L $Al_6O_{13}Si_2$ in Zn-10SiO_2 composite coating of mild steel respectively.

The decrease in wear rate of the composite coating may be attributed to higher load bearing capacity of hard $Al_6O_{13}Si_2$ material and better interfacial bond between the particle and the matrix reducing the possibility of particle pull out of which may result in lower wear. That is, increase in coating concentration increases its anti-wear activities by forming a more stable compound with the steel as a result of good movement of particle size distribution and uniformity at the interface [10, 13].

Also, it was noted that increase in the load exerted on the coated 10Zn-SiO_2 mild steel increases the rate of wear loss of the coated material. For instance, Zn-10$SiO_2$10$Al_6O_{13}Si_2$ had a wear loss of 0.005 g/min when 5 N load was exerted on the coated mild steel while the wear loss value was 0.007 g/min when a load of 10 N was exerted. As the force exerted increased, more stress is experienced by the mild steel due to the distortion of the intermolecular bonds within the mild steel, and the cumulative effect of this results in the gradual wearing away of the material [20].

3.4 Electrochemical test result of Zn-SiO_2 and Zn-SiO_2-$Al_6O_{13}Si_2$ deposited mild steel

Polarization examination was performed on Zn-SiO_2 alloy matrix to verify the corrosion rate, protective ability, and the reactivity of the deposited composite alloy in 3.65% NaCl environment. From Table 4 and Fig. 6 (the cathodic and anodic polarization curves for the composite coating matrix), the corrosion rate of the samples generally decreases as the concentration of $Al_6O_{13}Si_2$ increased from 0 to 15. The Zn-SiO_2 sample has a significant corrosion rate of 0.07000 mm/year due to absence of surface protection of $Al_6O_{13}Si_2$. Also, it can be seen that the anodic and cathodic processes of all the composite fabricated layer exhibit high corrosion resistance characteristic as revealed through a higher corrosion potential and lower current densities' when compared to Zn-SiO_2 sample. These facts justified the need for the coating of Zn-SiO_2 alloy with functional metals.

One noticeable observation is the progression of immunity of the composite coating to corrosion erosion and pitting behavior. It can be observed that the higher the concentration of $Al_6O_{13}Si_2$, the higher the corrosion-resistant properties of the coated mild steel. Zn-10SiO_2-15$Al_6O_{13}Si_2$ alloy was found to have produced improved polarization potential of − 1.1468 V, polarization resistance of 372.99 Ω, and corrosion rate of 0.01123 mm/year. Next to the best produced alloy is Zn-10SiO_2-10$Al_6O_{13}Si_2$ composite alloy with a slight potential lower than the formal − 1.1811 V, polarization resistance of 204.64 Ω, and corrosion rate of 0.02196 mm/year. This behavioral pattern among the three composite alloys suggests that 15 g/L $Al_6O_{13}Si_2$ particles incorporated in the fabricated Zn-10SiO_2 matrix prevent particle interaction with 3.65% NaCl in the environment, thereby producing the best corrosion resistance of the composite coatings in line with studied by [20].

4 Conclusion

Fabrication of ternary nanocomposite coating alloy containing Zn-10SiO_2 matrix was achieved on mild steel. It was observed

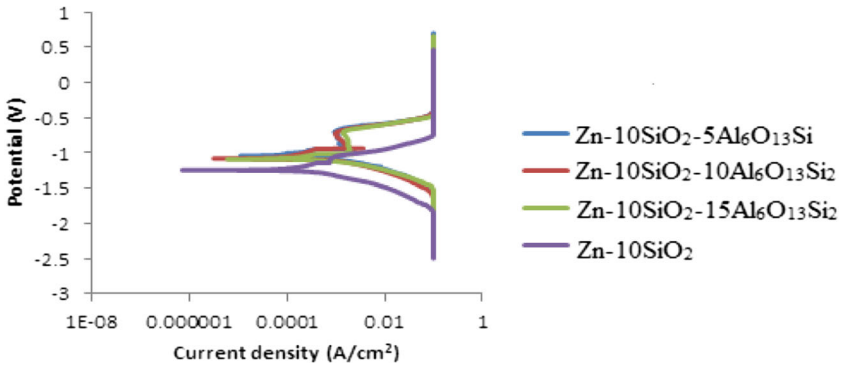

Fig. 6 Potentiodynamic polarization curves for Zn-SiO_2 and Zn-SiO_2-$Al_6O_{13}Si_2$ samples

that by modifying the composition of the electrolyte with additive, the produced structure displayed strong strengthening behavior with reduced grains as a result of dispersed composite particulate. Less agglomeration is form at the surface interface of Zn-10SiO_2. The effect of composition parameters and additive inclusion results into uniform dispersive crystal growth. The microhardness and tribological properties of the developed coating improved significantly from 98 HVN to 302 for Zn-10SiO_2-15$Al_6O_{13}Si_2$ alloy which is the overall best. The improvement in corrosion resistance was also significant with good resistance to chloride deformation. In all, it is good to mention that the corrosion properties revealed that the composite coatings have good anti-corrosion resistance properties.

References

1. Praveen BM, Venkatesha TV (2008) Electrodeposition and properties of Zn-nanosized TiO2 composite coatings. Appl Surf Sci 254: 2418–2424
2. Chuen-Chang L, Chi-Ming H (2006) J. Coat Technol Rese 3:99
3. Anawe PAL, Raji O, Fayomi OSI (2017) Procedia Manuf 7(2017): 562–566
4. Anawe PAL, Fayomi OSI, Popoola API (2017) Der Pharma Chem 9(9):36–42
5. Fayomi OSI, Popool API (2013) Int J Electrochem Sci 8:11502
6. Mohankumar C, Praveen K, Venkatesha V, Vathsala K, Nayana O (2012) J Coat Techno Rese 9:71
7. Abou-Krisha MM, Assaf FH, El-Naby SA (2009) Electrodeposition behavior of zinc–nickel–iron alloys from sulfate bath. J Rese Coat Technol 6:391–399
8. Rahman MJ, Sen SR, Moniruzzaman M, Shorowordi KM (2009) J. Mech Eng 40:9
9. Olafadehan OA, Ayoola AA, Akintunde OO, Adeniyi VO (2015) J Eng Sc Tech 10:633
10. Xu R, Wang J, GUO Z, Wang H (2008) Effects of rare earth on microstructures and properties of Ni-W-P-CeO2-SiO2 nanocomposite coatings. J Rare Earth 26:579–583
11. Ayoola AA, Efeovbokhan VC, Bafuwa OT, David OT (2014) Int J Sc Tech 4:66
12. Wang TG, Jeong D, Liu Y, Lyengar S, Melin S, Kim KH (2012) Study on nanocrystalline Cr2O3 films deposited by arc ion plating: II. Mechanical and tribological properties. J Surf Coat Technol 206: 2638–2644
13. Hammami O, Dhouibi L, Bercot P, Rezrazi EM, Triki E (2012) Int J Corro Sci 8:1
14. Shibli SMA, Chacko F, Divya C (2010) Al2O3–ZrO2 mixed oxide composite incorporated aluminium rich zinc coatings for high wear resistance. J Corros Sci 52:518–525
15. Gomes A, Frade T, Nogueira ID (2012) Curr. Micros. Contri. Advan. Sci Technol 2:1146
16. Fayomi OSI, Abdulwahab M, Popoola API (2013) J Ovonic Rese 9:123
17. Zhang Y, Huang B, Li P, Wang X, Zhang Y (2013) J. Euro Ceram Soc 58:7
18. Abdel A, Barakat MA, Mohamed RM (2008) Electrophoreted Zn–TiO2–ZnO nanocomposite coating films for photocatalytic degradation of 2-chlorophenol. Appl Surf 254:4577–4583
19. Su YL, Kao WH (2003) Trib Int 36:11
20. Dong D, Chen XH, Xiao WT, Yang GB, Zhang PY (2009) Preparation and properties of electroless Ni–P–SiO2 composite coatings. Appl Surf Sci 255:7051–7055
21. Popoola API, Fayomi OSI, Popoola OM (2012) Int J Electrochem Sci 7:4898
22. Popoola API, Fayomi OS (2011) Effect of some process variables on zinc coated low carbon steel substrates. Sci Res Essay 6:4264–4272
23. Subramanian B, Mohan S, Jayakrishnan S (2006) Structural, microstructural and corrosion properties of brush plated copper–tin alloy coatings. Surf Coat Technol 201:1145–1151
24. Fayomi OSI, Popoola API (2013) Rese. Chem. Int. 39:N06. https://doi.org/10.1007/s11164-013-1354-2
25. Frade T, Bouzon Z, Gomes A, Da Silva MI, Pereira MI (2010) Pulsed-reverse current electrodeposition of Zn and Zn-TiO2 nanocomposite films. Surf Coat Technol 204:3592–3598
26. Arici M, Nazir H, Aksu A (2011) Investigation of Sn–Zn electrodeposition from acidic bath on EQCM. J Alloys Comp 509:1534–1537
27. Fayomi OSI, Popoola API (2012) An Int J Electro Sci 7:6555–6570
28. Z., Dong, X., Peng, Y., L. Guan, Li, F. Cor Sci, 62 (2012), 147–152
29. Anawe PAL, Fayomi OSI (2017) Investigation of microstructural and physical characteristics of nano composite tin oxide-doped Al 3+ in Zn 2+ based composite coating by DAECD technique. Results Physics 7:777–788
30. Anawe PAL, Fayomi OSI (2017) Impact of applied potential on the structural and non-lubricated wear composite coating in petrochemical industry. Port Electrochim Acta 35(5):297–303
31. PAL Anawe, O Raji, O. S. I. Fayomi, V. Efeovobohkan. 2017. Procedia Manuf 7 (2017) 556–561